Low phosphate represses histone deacetylase complex1 to regulate root system architecture remodeling in *Arabidopsis*

Jia Meng Xu[1,2], Zhan Qi Wang[3], Jia Yi Wang[1], Peng Fei Li[1], Jian Feng Jin[1], Wei Wei Chen[4], Wei Fan[5], Leon V. Kochian[6] (iD), Shao Jian Zheng[1] (iD) and Jian Li Yang[1] (iD)

[1]State Key Laboratory of Plant Physiology and Biochemistry, College of Life Sciences, Zhejiang University, Hangzhou 310058, China; [2]The Key Laboratory of Plant Cell Engineering and Germplasm Innovation, Ministry of Education, College of Life Science, Shandong University, Jinan 250100, China; [3]Key Laboratory of Vector Biology and Pathogen Control of Zhejiang Province, College of Life Sciences, Huzhou University, Huzhou 313000, China; [4]Research Centre for Plant RNA Signaling, College of Life and Environmental Sciences, Hangzhou Normal University, Hangzhou 310036, China; [5]College of Resources and Environment, Yunnan Agricultural University, Kunming 650201, China; [6]Global Institute for Food Security, University of Saskatchewan, Saskatoon, SK S7N 4J8, Canada

Summary

- The mechanisms involved in the regulation of gene expression in response to phosphate (Pi) deficiency have been extensively studied, but their chromatin-level regulation remains poorly understood.
- We examined the role of histone acetylation in response to Pi deficiency by using the *histone deacetylase complex1* (*hdc1*) mutant. Genes involved in root system architecture (RSA) remodeling were analyzed by quantitative real-time polymerase chain reaction (qPCR) and chromatin immunoprecipitation qPCR.
- We demonstrate that histone H3 acetylation increased under Pi deficiency, and the *hdc1* mutant was hypersensitive to Pi deficiency, with primary root growth inhibition and increases in root hair number. Concomitantly, Pi deficiency repressed HDC1 protein abundances. Under Pi deficiency, *hdc1* accumulated higher concentrations of Fe^{3+} in the root tips and had higher expression of genes involved in RSA remodeling, such as *ALUMINUM-ACTIVATED MALATE TRANSPORTER1* (*ALMT1*), *LOW PHOSPHATE ROOT1* (*LPR1*), and *LPR2* compared with wild-type plants. Furthermore, Pi deficiency enriched the histone H3 acetylation of *ALMT1* and *LPR1*. Finally, genetic evidence showed that LPR1/2 was epistatic to HDC1 in regulating RSA remodeling.
- Our results suggest a chromatin-level control of Pi starvation responses in which HDC1-mediated histone H3 deacetylation represses the transcriptional activation of genes involved in RSA remodeling in *Arabidopsis*.

Introduction

Phosphorus (P) is essential for plant growth and development (Marschner, 1995). Plants absorb P from the soil in the form of inorganic phosphate (Pi), whose bioavailability is often limited in many ecosystems because of its low solubility and mobility in soil (Holford, 1997). In order to overcome Pi limitation, plants have evolved Pi starvation responses (PSRs) that involve developmental, physiological and biochemical changes to increase Pi acquisition and use efficiency.

Considerable progress has been made towards unraveling the molecular mechanisms of PSRs, which have been classified into two partially independent signaling pathways, namely local and systemic responses (Gutiérrez-Alanís *et al.*, 2018). The MYB transcription factors (TFs) PHOSPHATE STARVATION RESPONSE1 (PHR1) and PHR1-like (PHL1) are central integrators in the transcriptional regulation of the majority of PSR genes (Bustos *et al.*, 2010). Other TFs acting as transcriptional

activators or repressors of PSR have also been identified in plants (Devaiah *et al.*, 2007; Chen *et al.*, 2009; Wang *et al.*, 2014; Su *et al.*, 2015). Although systemic responses to Pi deficiency depend mostly on PHR1 and related TFs, local responses are independent of the function of these TFs. Controlled by local extracellular Pi availability, the remodeling of root system architecture (RSA), which includes the inhibition of primary root growth, increase in lateral root number, and growth and enhancement of root hair density, shows major developmental changes in response to Pi deficiency. Additionally, increased accumulation of iron (Fe) is essential for the Pi deficiency-induced inhibition of primary root growth (Svistoonoff *et al.*, 2007; Ward *et al.*, 2008), and aspects of the molecular basis of this response have recently been identified as described in the following. However, there is still much to learn about the molecular basis of PSRs.

It is now recognized that the extracellular Pi sensing mechanism is based on the relationship between P deficiency and root Fe accumulation. The Fe : Pi ratio determines the concentration of

reactive oxygen species (ROS) in the root apoplast (Abel, 2017). Several components involved in root tip Fe accumulation and redistribution to regulate the remodeling of RSA have been identified. *Arabidopsis pdr2* (*phosphate deficiency responses2*) exhibits greater inhibition of primary root growth than do wild-type (WT) plants under Pi deficiency (Ticconi *et al.*, 2004). By contrast, *LPR1* (*LOW PHOSPHATE ROOT1*) and its paralog, *LPR2*, are insensitive to Pi deficiency-induced inhibition of primary root growth (Svistoonoff *et al.*, 2007). *PDR2* encodes a P5-type ATPase, whereas LPR1/2 is a ferroxidase, which enables ROS generation and callose deposition in both the apoplast surrounding the stem cell niche (SCN) of the root apical meristem (RAM) and the root transition zone. In another recent work, the *Arabidopsis* mutant *hsp10* (*hypersensitive to Pi starvation10*) displayed increased inhibition of primary root growth and enhanced production of lateral roots under Pi deficiency (Dong *et al.*, 2017). The *hsp10* allele is a loss-of-function allele of *ALUMINUM SENSITIVE3* (*ALS3*), which encodes a half-size ABC transporter involved in Al resistance (Xu *et al.*, 2019). *ALS3* and its interacting partner, *AtSTAR1* (*Sensitive To Aluminum Rhizotoxicity1*), have been shown to be involved in RSA remodeling under Pi deficiency (Belal *et al.*, 2015; Dong *et al.*, 2017). Recently, it was also reported that mutants of other Al tolerance genes, *stop1* and *almt1*, are both insensitive to Pi deficiency in terms of primary root growth inhibition (Balzergue *et al.*, 2017; Mora-Macías *et al.*, 2017). STOP1 is a zinc-finger TF that regulates Al resistance by transcriptionally activating *ALMT1* expression (Iuchi *et al.*, 2007; Tokizawa *et al.*, 2015). Interestingly, genetic analysis showed that LPR1/2 is epistatic to other identified components involved in RSA remodeling, although LPR1/2 is subjected to transcriptional regulation in response to Pi deficiency. However, how LPR1/2 is transcriptionally regulated and whether other components are involved in RSA remodeling in response to Pi deficiency are still unknown.

Transcription occurs in the context of chromatin, a highly condensed structure in which the DNA is wrapped around nucleosomes composed of histones H2A/B, H3 and H4, and further stabilized by the linker histone H1 (Over & Michaels, 2014; Hergeth & Schneider, 2015). Recent evidence suggests that substantial regulation of cellular Pi homeostasis occurs at the histone level. For example, the nuclear actin-related protein, ARP6, which is an essential component of the SWR1 chromatin remodeling complex, is involved in regulating PSR gene expression by mediating the deposition of histone variant H2A.Z at these genes (Smith *et al.*, 2010). Further, in an incomplete loss-of-function mutant *atipk1-1*, the transcriptional increase in a number of PSR genes is correlated with the reduction of H2A.Z occupation in chromatin (Kuo *et al.*, 2014). Recently, a reverse genetics approach identified HDA6, HDA9 and HDA19, the class I members of the histone deacetylase (HDAC) family, as being involved in both root cell length and expression regulation of some Pi-responsive genes under Pi-deficiency conditions (Chen *et al.*, 2015). HDACs catalyze the histone deacetylation of Lys residues on H3 and H4, which establishes a repressive mark for gene expression (Kouzarides, 2007; Roudier *et al.*, 2009). Therefore, reversible histone acetylation is likely to be involved in RSA remodeling under Pi deficiency.

In the present study, we used a *histone deacetylase complex1* (*hdc1*) mutant to investigate the role of histone acetylation in RSA remodeling in response to Pi deficiency in *Arabidopsis*. We found that *hdc1* displayed increased inhibition of primary root growth under Pi deficiency in comparison to the WT plants, which coincided with LPR1/2-mediated Fe^{3+} deposition in the root tips. We further demonstrated that HDC1 was subjected to post-transcriptional downregulation by Pi deficiency, which in turn resulted in transcriptional activation of core genes upstream of LPR1/2. In addition, genetic analysis showed that LPR1/2 was epistatic to HDC1. Taken together, our results suggest that HDC1 is a negative regulator of RSA remodeling under Pi deficiency.

Materials and Methods

Plant materials

All *Arabidopsis thaliana* materials used in this study were of the Columbia-0 ecotype (Col-0). The T-DNA insertion mutant line *hdc1* (GABI-Kat 054G03) is a previously reported knockout mutant (Perrella *et al.*, 2013). Both *lpr1* (SALK_016297) and the *lpr1lpr2* double mutants were kind gifts from Dr Dong Liu (Tsinghua University, China). The *hdc1lpr1* and *hdc1lpr1lpr2* mutants were generated by genetic crosses between *hdc1* and *lpr1* or *lpr1lpr2*, respectively. The sequences of all the primers used for the homozygous offspring verification are listed in Supporting Information Table S1.

Plant growth conditions

The *Arabidopsis* seeds were surface-sterilized with 75% ethanol for 5 min, washed thoroughly with sterile water, and placed at 4°C in darkness for 3 d. Then, the seeds were sown onto Petri dishes containing different modified medium based on ½ Murashige & Skoog (½ MS). The Petri dishes with the seeds were placed vertically in a plant incubator at 22°C, at 70% relative humidity, with a light intensity of 130 μmol $m^{-2}s^{-1}$ and a 16 h : 8 h, light : dark photoperiod.

The +Pi growth medium (pH 5.8) consisted of 1/2 MS medium containing 625 μM Pi, 1% Suc, and 0.8% agar (Sigma). The −Pi medium (pH 5.8) consisted of 1/2 MS medium supplemented with 10 μM Pi, 1% Suc (pH 5.8), with the equivalent K (supplied by KH_2PO_4) replaced with K_2SO_4 and solidified with 1% agarose (Biowest Regular Agarose G-10; Biowest, Barcelona, Spain). For the −Pi–Fe experiment, Fe^{2+} was omitted from the −Pi medium.

For the hydroponics, we used a modified one-fifth nutrient solution (Zheng *et al.*, 2005) with 200 μM (+Pi) or 1 μM (−Pi) $NH_4H_2PO_4$. In the −Pi treatment, the missing NH_4^+ (supplied by $NH_4H_2PO_4$) was replaced with $(NH_4)_2SO_4$.

Construction of Arabidopsis transgenic lines

A DNA sequence containing a 646 bp *HDC1* promoter sequence and the genomic coding sequence was amplified from WT genomic DNA using the primers designed to contain the *Bam*HI

and *Kpn*I restriction enzyme sites (Table S1). After digestion, the fragment was ligated to pCAMBIA1300 to generate the $HDC1_{pro}::HDC1_{gDNA}$-GFP recombinant plasmid and then transformed into the *hdc1* mutant mediated by *Agrobacterium* to obtain the complementation lines.

To generate the *HDC1pro::GUS* construct, the promoter sequence of the *HDC1* gene was amplified from *Arabidopsis* genomic DNA (Table S1). The purified fragment was then inserted into the pBI101.3-GUSplus vector with a β-glucuronidase (GUS) reporter gene fused into the 3′ end of the 646 bp promotor region. The *HDC1_{pro}::GUS* construct was introduced into *Agrobacterium* strain GV3101 and then transformed into Col-0 by the floral dip method. The transgenic plants were selected on MS plates containing 50 mg l^{-1} kanamycin, and the presence of the transgene was further verified by PCR. The homozygous line with a strong phenotype was selected for the analysis.

To construct the *ALMT1_{pro}::GUS* and *LPR1_{pro}::GUS* transgenic lines, 2490 and 2503 bp promoter sequences of *ALMT1* and *LPR1*, respectively, were cloned into the pCAMBIA1301 vector to obtain the *ALMT1_{pro}::GUS* and *LPR1_{pro}::GUS* constructs. Each plasmid was introduced into both the WT and *hdc1* mutant to generate the GUS reporter lines.

Western blot

Sodium dodecyl sulphate (SDS)-polyacrylamide gel electrophoresis was performed according to Laemmli (1970). The proteins were solubilized in SDS loading buffer and separated on a 12.5% (w/v) acrylamide gel with the Mini-PROTEAN Tetra System (Bio-Rad). After electrophoresis, the separated proteins were electrotransferred to a polyvinylidene fluoride membrane with the Mini Trans-Blot System (Bio-Rad). Anti-acetyl-H3 (06-599; Merck-Millipore, Darmstadt, Germany) and anti-acetyl-H4 (06-598; Merck-Millipore) antibodies (1 : 3000 dilution) were added and incubated with the membrane for 90 min at room temperature. An anti-actin antibody (Sigma) was used to normalize the loading quantity of the proteins. A secondary goat anti-rabbit antibody (AP156P; Merck-Millipore) or goat anti-mouse antibody (Ab205719; Abmart, Berkeley Heights, NJ, USA) conjugated with horseradish peroxidase (HRP) was used at a dilution of 1 : 5000. Western blot signals were detected by the Luminata^{TM} Western HRP Substrate Kit (Merck-Millipore).

RT-PCR and quantitative real-time PCR

Four-day-old seedlings were transferred onto the +Pi or −Pi media for 2 d, and then the 2–3 mm segments of the root tips were excised for RNA isolation. RNA extraction was performed using the MiniBEST Universal RNA Extraction Kit (Takara, Dalian, China). First-strand cDNA was synthesized from 1 μg of total RNA using the PrimeScript^{TM} RT Master Mix Kit (Takara). Quantitative real-time PCR was carried out on a LightCycler480 machine (Roche Diagnostics, Basel, Switzerland) using SYBR$^{®}$ Premix Ex Taq (Takara). *Actin2* and *UBQ10* were used as internal controls. The primers are listed in Table S1.

To examiine whether the *hdc1* mutant harbored a null *HDC1* gene, semiquantitative reverse transcription polymerase chain reaction (RT-PCR) was performed. *UBQ1* (as the internal control) and *HDC1* cDNA were amplified using rTaq DNA polymerase with the primers listed in Table S1. PCR was carried out as follows: 94°C for 3 min, 26 (*HDC1*) or 24 cycles (*UBQ1*) of 94°C denaturing for 30 s, 56°C annealing for 1 min and 72°C extension for 30 s, and a final 5 min extension at 72°C.

Fe histochemical staining

Iron accumulation in the root tips was detected by using Perls staining according to Roschzttardtz *et al.* (2009). Four-day-old seedlings were transferred onto the +Pi or −Pi medium for 2 d, and then the roots were excised to be incubated in 4% (v/v) HCl and 4% (w/v) K-ferrocyanide for 15 min. The roots were washed with deionized water three times to stop the staining reaction and cleared with chloral hydrate (1 g ml^{-1}, 15% glycerol) for observation with a Nikon AZ100 microscope.

For diaminobenzidine (DAB) intensification, the root samples after Perls staining were incubated in methanol containing 10 mM Na-azide and 0.3% (v/v) H$_2$O$_2$ for 60 min. The samples were washed with 100 mM Na phosphate buffer (pH 7.4) and then incubated for 5 min in the same buffer containing 0.025% (w/v) DAB (Sigma-Aldrich) and 0.005% (v/v) H$_2$O$_2$. The reaction was stopped by washing the samples with deionized water. The stained samples were cleared in chloral hydrate (1 g ml^{-1}, 15% glycerol) and then analyzed with a Nikon AZ100 microscope.

GUS assay

Four-day-old GUS reporter transgenic seedlings were transferred to the +Pi or −Pi medium for 2 d, and then GUS staining was performed according to Jefferson *et al.* (1987) with minor modifications. The staining solution (10 ml) consisted of 5 ml phosphate buffer (50 mM, pH 7.0), 0.2 ml EDTA (0.5 M, pH 8.0), 0.1 ml potassium ferricyanide (50 mM), 0.1 ml potassium ferrocyanide (50 mM), 0.1 ml 10% TritonX-100, 10–20 mg X-Gluc, and ddH$_2$O for a total volume of 10 ml and was stored at 4°C until use. The stained seedlings were observed and photographed with a Nikon AZ100 microscope.

Determination of Pi and Fe

Determination of Pi content was done using the molybdenum blue method described previously (Delhaize & Randall, 1995; Chen *et al.*, 2011). Seven-day-old Arabidopsis seedlings were transferred onto the +Pi or −Pi medium for 7 d, and the roots and shoots were collected for Pi content analysis using a continuous-flow analyzer (San plus system; Skalar, Breda, the Netherlands).

Iron content was determined by the following method description. The roots were harvested from the Arabidopsis seedlings treated on the +Pi or −Pi medium for 7 d, washed in deionized water three or four times, and the excess surface water was then

removed so that the roots could be weighed. The root samples were digested with HNO_3 and the Fe content was determined by inductively coupled plasma-atomic emission spectrometry (IRIS/AP optical emission spectrometer, Thermo Jarrell Ash, Franklin, MA, USA).

Confocal microscopy and meristem cell number counting

The plants were immersed in propidium iodide solution (10 mg ml^{-1}) for 1 min, and washed with deionized water for 2 min. The roots were then observed using a confocal laser scanning microscope (Zeiss LSM710). The excitation and emission wavelengths were 536 and 620 nm, respectively. The meristem cell number was counted based on the files of cortex cells from the quiescent center to the first elongated cell.

ChIP-qPCR

A chromatin immunoprecipitation (ChIP) assay was conducted as described previously with minor modifications (Gendrel *et al.*, 2005; Perrella *et al.*, 2013). The *Arabidopsis* seeds were sown on a plastic mesh floating in a nutrient solution. Four-day-old hydroponically cultured *Arabidopsis* plants were transferred to the +Pi or −Pi solution for 2 d. Then 0.8 g of the roots were harvested and incubated in 1% (w/v) formaldehyde for 15 min under vacuum conditions. After stopping the cross-linking with 1.25 mM glycine, the chromatin complexes with the proteins were extracted, sonicated, precipitated with immunoglobulin G (as a negative control), incubated with the anti-acetyl-H3 (06-599; Merck-Millipore) antibody at 4°C overnight, and then captured with Magna ChIP™ Protein A + G Magnetic Beads (16-663; Merck-Millipore). The beads were washed before the reverse cross-linking of the immunoprecipitated chromatin DNA (ChIP DNA) and the input chromatin DNA, and then the proteins were digested and the DNA was purified. The immunoprecipitated DNA was determination by quantitative RT-PCR (qRT-PCR) with the primers listed in Table S1. ChIP enrichment was normalized with input from a nonprecipitated sample.

Accession numbers

Sequence data from this article can be found in The Arabidopsis Information Resource database under the following accession numbers: HDC1 (At5g08450), LPR1 (At1g23010), LPR2 (At1g71040), ALMT1 (At1g08430), STOP1 (At1g34370), PDR2 (At4g15230), PT2 (At2g38940).

Results

### HDC1 derepresses primary root growth under Pi deficiency

To investigate whether histone acetylation modifications are involved in PSRs in *Arabidopsis*, we first quantified the acetylated histones H3 and H4 in response to Pi deficiency in the roots of WT *Arabidopsis*. Pi deficiency induced a dramatic increase in the acetylated histone H3 but had a minor effect on the acetylation

of histone H4 (Fig. S1), suggesting that acetylation activation or the repression of deacetylation primarily occurs on histone H3 under Pi-deficient conditions. It was reported that the *hdc1* mutant has higher levels of the acetylated form of H3 than the deacetylated form in *Arabidopsis* leaves (Perrella *et al.*, 2013). Here, we further demonstrated that the roots of *hdc1* showed higher acetylation of H3 than did the roots of the WT plants, irrespective of Pi status (Fig. 1a). Thus, *hdc1* is a useful mutant for investigating the role of histone H3 acetylation in PSRs in *Arabidopsis*. RT-PCR analysis showed that the *HDC1* transcript was undetectable in the *hdc1* mutant, confirming that *hdc1* is a knockout mutant (Fig. 1b). We subsequently developed two complementation lines carrying *HDC1* genomic DNA fused with green fluorescence protein (GFP) under the control of the *HDC1* promoter transformed into the *hdc1* background (*HDC1pro::HDC1gDNA::GFP/hdc1*). *HDC1* transcripts were detected in both complementation lines (Fig. 1b). Western blot analysis showed that the acetylated H3 levels were induced by Pi deficiency in both of the complementation lines (Fig. S2), suggesting that HDC1 was functioning normally in both complementation lines. Consistent with a previous report (Perrella *et al.*, 2013), the *hdc1* mutant had a slightly shorter primary root compared with the WT *Arabidopsis* under Pi-sufficient conditions (Fig. 1c,d). However, under Pi-deficient conditions, the *hdc1* mutant displayed significantly greater primary root growth inhibition compared with the WT plants (Fig. 1c,e). From 2 d after germination (DAG), the growth of the primary root ceased in the *hdc1* mutant (Fig. 1e), but continued to elongate in the WT plants and also in the two complementation lines (Fig. 1e). At 7 DAG, the primary root length of *hdc1* was only 20% of that in the WT plants (Fig. 1e). In addition, Pi deficiency stimulated root hair production in all genotypes (Fig. S3a), but the number was significantly higher in the *hdc1* mutant than in the others (Fig. S3b). However, the root hair length did not differ among them irrespective of Pi status (Fig. S3c). These results suggest that HDC1 is involved in the Pi deficiency-induced inhibition of primary root growth, one of the hallmark responses to Pi deficiency (Abel, 2017).

HDC1 derepresses primary root growth by inhibiting cell elongation

A previous study showed that the inhibition of primary root growth occurred within several hours under Pi deficiency (Balzergue *et al.*, 2017). Root growth is caused by both cell elongation and cell division. To investigate which process is involved in HDC1-regulated root growth depression in response to Pi deficiency, we performed a time-course experiment. The growth of the primary root was significantly inhibited by 1 d of Pi deficiency, but the inhibition was more severe in the *hdc1* mutant (Fig. 2a). Furthermore, the relative root elongation was progressively decreased by Pi deficiency in both the WT and *hdc1* mutant plants with prolonged treatment (Fig. S4). By contrast, although the meristem cell number was also affected by Pi deficiency in both the WT and *hdc1* mutant plants, there was no difference between them irrespective of Pi status (Fig. 2c).
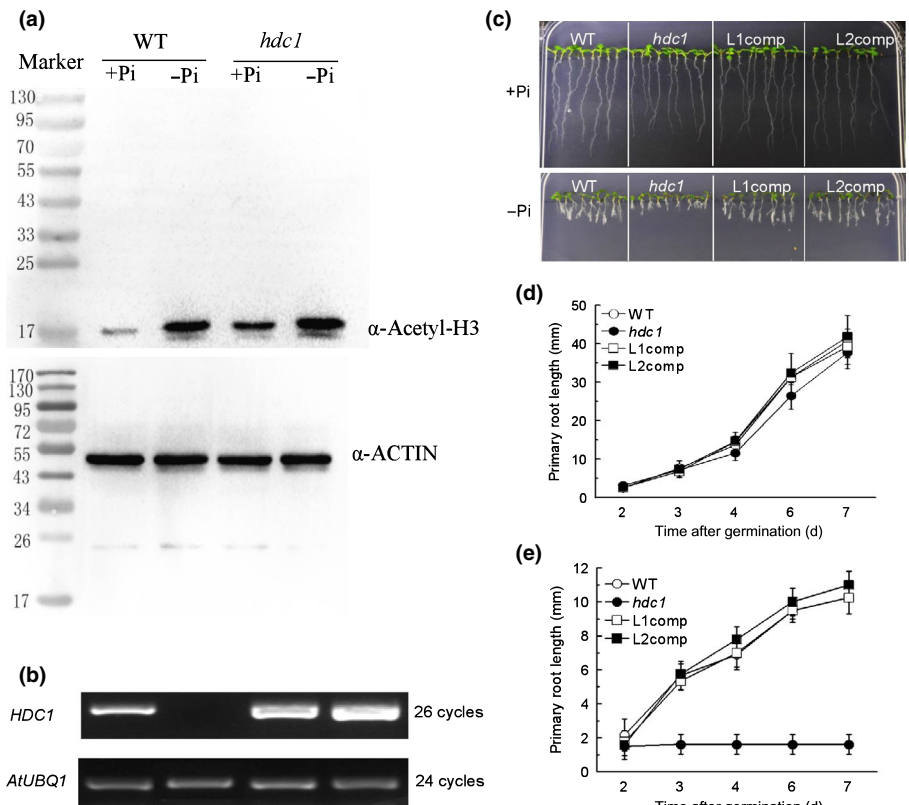
Fig. 1 HDC1 represses phosphate starvation responses in *Arabidopsis thaliana*. (a) Western blot analysis of histone H3 acetylation of Arabidopsis wild-type (WT) and *hdc1* mutant roots subjected to inorganic phosphate (Pi)-sufficient or -deficient conditions for 2 d. (b) Reverse transcription polymerase chain reaction detection of *HDC1* expression in WT, *hdc1* and two complementation lines carrying genomic DNA of *HDC1* fused with green fluorescence protein (GFP) reporter proteins driven by its own promoter. (c) Phenotype of seedlings of WT, *hdc1* and complementation lines grown on +Pi or −Pi medium for 7 d after germination (DAG). (d, e) Root length of seedlings of WT, *hdc1* and complementation lines grown on +Pi (d) or −Pi (e) medium from 2 to 7 DAG. Data are means ± SD (*n* = 8).

Moreover, the meristem cell number did not decrease further after 1 d of Pi deficiency (Fig. 2c). Therefore, the inhibition of cell elongation was the primary reason for root growth inhibition in the *hdc1* mutant, albeit Pi deficiency decreased both cell elongation and cell division.

HDC1 is downregulated by Pi deficiency at the post-transcriptional level

Phosphate deficiency-induced inhibition of primary root growth is a local response controlled by extracellular Fe and Pi concentrations around the root tip (Sánchez-Calderón *et al.*, 2005). We thus analyzed the tissue-specific expression of *HDC1* using *in planta* promoter-GUS activity assays. *Arabidopsis* plants stably expressing the *GUS* reporter gene under the control of the *HDC1* promoter showed that *HDC1* was ubiquitously expressed in vegetative seedlings (Fig. 3a). However, GUS activity was stronger in the root tip than in other parts of the root (Fig. 3a), consistent with a possible role of *HDC1* in root tip responses to Pi deficiency. The observation that *hdc1* exhibited hypersensitivity to Pi deficiency in terms of primary root growth inhibition prompted us to investigate the expression of *HDC1* in response to Pi deficiency. We first examined the expression level of *HDC1* in the roots during Pi deficiency. As depicted in Fig. 3(b), *HDC1* transcript abundance was not affected by Pi deficiency in comparison to the plants grown under sufficient Pi, suggesting that HDC1 may be subjected to post-transcriptional regulation by Pi availability. Therefore, we examined *HDC1-GFP* protein changes in our complementation lines in response to Pi availability.

Confocal microscopy of the root tips revealed nuclear localization of HDC1-GFP under Pi-sufficient conditions (Fig. 3c), which, interestingly, diminished in the roots grown under Pi-deficient conditions (Fig. 3c,d). Western blot analysis confirmed that the abundances of the HDC1-GFP fusion proteins were dramatically reduced by Pi deficiency (Fig. 3e). Interestingly, a 26S proteasome inhibitor, MG132, repressed the degradation of the HDC1-GFP fusion proteins, suggesting that HDC1 is subjected to 26S proteasome-mediated degradation under Pi deficiency (Fig. 3e). These results indicate that HDC1 is post-translationally regulated in response to Pi deficiency.

Overaccumulation of Fe^{3+} is responsible for hdc1 mutant phenotypes

Studies have shown that the inhibition of primary root growth under Pi deficiency involves triggering high Fe accumulation in the roots (Ward *et al.*, 2008). We therefore examined the concentration of Fe in the roots using the Perls staining method, which mainly stains labile (nonheme) Fe^{3+} (Meguro *et al.*, 2007). In both the WT and *hdc1* mutant plants grown on Pi-sufficient medium, the blue staining of Fe^{3+} was mainly localized in the SCN within the RAM (Fig. 4). On the −Pi medium, Fe^{3+} accumulation in the SCN of the WT plants was dramatically reduced, and light-blue staining was evident mostly in the root maturation zone, suggesting that Pi deficiency induced Fe accumulation in the maturation zone or the basipetal redistribution of Fe. Notably, the blue staining was much stronger in the *hdc1* mutant than in the WT plants, in both the root tip and maturation zone.
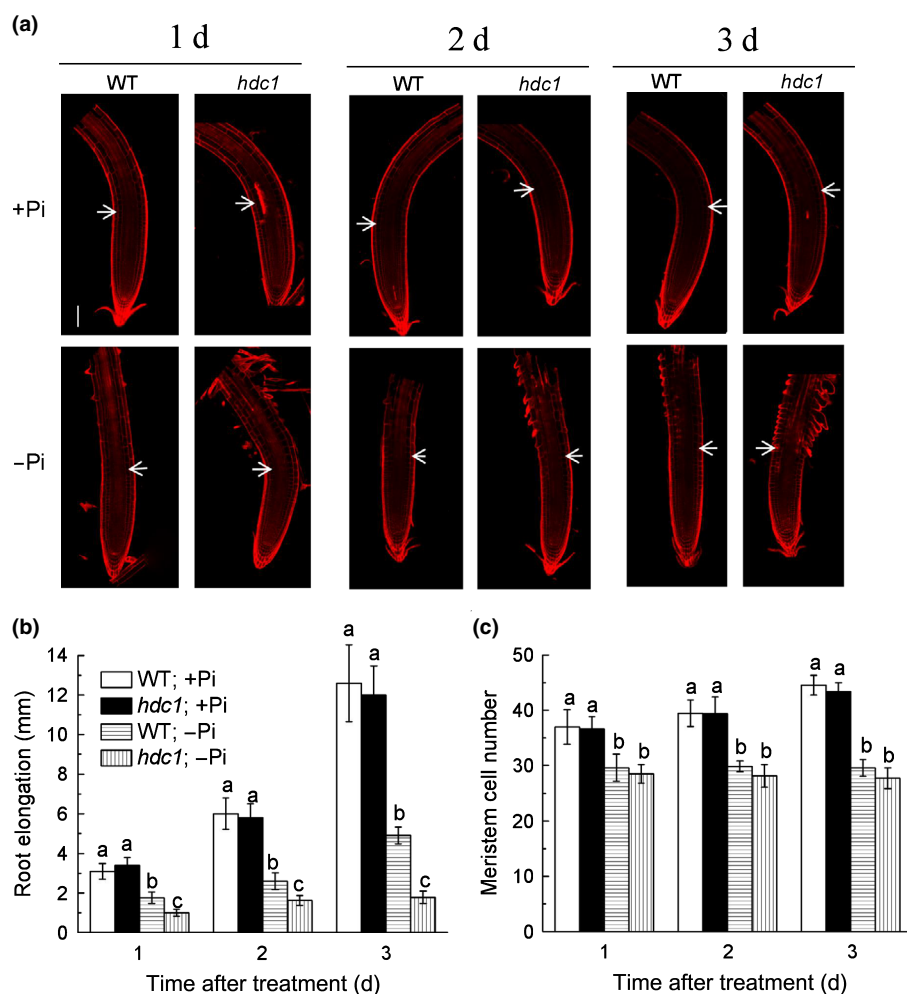
Fig. 2 Effect of inorganic phosphate (Pi) deficiency on primary root elongation and meristem cell number in wild-type (WT) and *hdc1* mutant *Arabidopsis thaliana* plants. Four-day-old seedlings of WT and *hdc1* were subject to Pi deficiency or Pi sufficiency for 3 d. (a) Confocal images of root tips of WT and *hdc1* plants with propidium iodide staining. White arrows indicate the position above which is the first elongated cell. Bar, 100 μm. (b) Elongation of primary root of WT and *hdc1* plants. (c) Number of meristem cells. The cortex cell number between the quiescent center and the first elongated cell was countered. Data are means ± SD ($n = 8$). Different letters indicate significant differences (Tukey test, $P < 0.05$).

However, this intensified Fe accumulation was reduced to the amount seen in roots of the WT plants in both of the complementation lines. A more sensitive Perls/DAB staining method, which stains both Fe^{2+} and Fe^{3+} (Roschzttardtz *et al.*, 2009), also showed similar Fe accumulation and distribution patterns (Fig. S5).

To further verify whether the intensified inhibition of primary root growth in the *hdc1* mutant under Pi-deficiency conditions involved Fe overaccumulation in the root tip, we omitted Fe from the −Pi medium to analyze the Pi-deficiency root growth responses in *hdc1*. Whereas root growth was remarkably inhibited by Pi deficiency with the presence of Fe in the growth medium, the primary root length under the −Pi−Fe conditions was the same as in the plants grown under Pi-sufficient conditions in all lines (Fig. 5a,c). Consistent with the recovered primary root growth, the Perls and Perls/DAB staining assays indicated that there was no Fe accumulation in the roots of the different *Arabidopsis* genotypes studied here under the −Pi−Fe condition (Fig. 5b).

In addition, we used ICP-OES to analyze the Fe content in the roots of both WT and *hdc1* plants subjected to external Pi. Under Pi-sufficient conditions, there was no significant difference in the Fe content of the roots between the WT and *hdc1* mutant plants.

Although Pi deficiency increased the root Fe accumulation in both the WT and *hdc1* plants, it was much higher in the roots of *hdc1* than in the roots of the WT (Fig. 6a). However, there was no difference in the Pi content in the roots and shoots between the WT and the *hdc1* mutant under the +Pi or −Pi conditions (Fig. 6b), suggesting that the increased inhibition of primary root growth of *hdc1* under Pi deficiency did not significantly impact plant Pi homeostasis. Overall, these results indicate that increased inhibition of primary root growth in *hdc1* is associated with root Fe hyperaccumulation.

HDC1 negatively regulates the expression of genes involved in RSA remodeling under Pi deficiency

The observation that *hdc1* hypersensitivity to Pi deficiency contributed to root Fe^{3+} overaccumulation led us to hypothesize that HDC1 could modulate RSA remodeling under Pi deficiency through the transcriptional regulation of some previously identified genes to play a role in PDR-associated root architecture changes. To this end, we analyzed the expression level of genes involved in RSA remodeling in both the WT and *hdc1*. If HDC1 acts as a modulator linking Pi deficiency to the transcriptional activation of downstream responsive genes, we infer that the
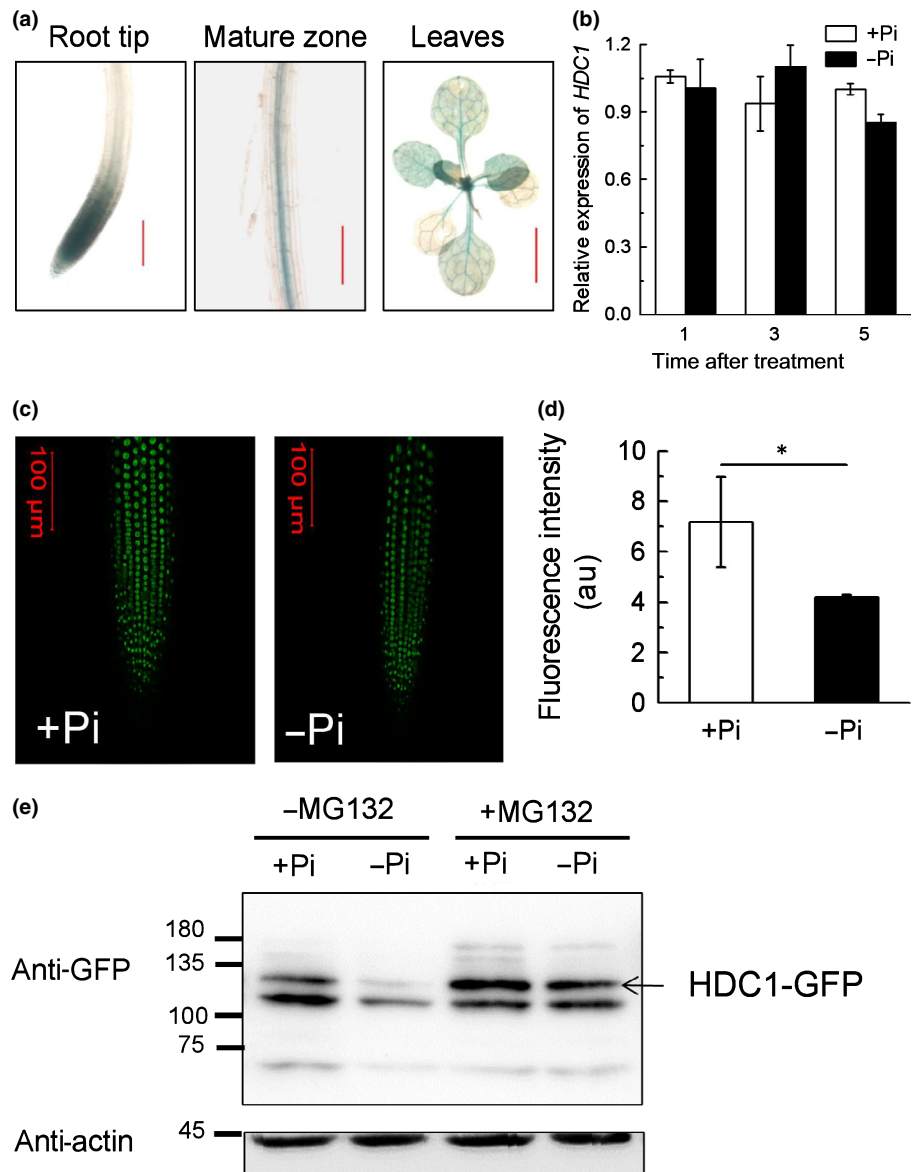
Fig. 3 Expression patterns of *HDC1* in response to inorganic phosphate (Pi) deficiency in *Arabidopsis thaliana*. (a) β-Glucuronidase (GUS) activity assay of *HDC1* expression. Bars, 100 μm (roots); 1 cm (leaves). (b) Quantitative reverse transcription polymerase chain reaction (qRT-PCR) analysis of time course of *HDC1* expression in the root in response to Pi deficiency. Four-day-old seedlings of wild-type (WT) plants were transferred to either +Pi or −Pi medium for different amounts of time. Expression levels were normalized to the expression of an internal control, *AtACT2*. Data are means ± SD (*n* = 3). (c) Green fluorescence protein (GFP)-fluorescence of HDC1-GFP in root tips. Four-day-old seedlings of *hdc1* complementation lines were transferred to either +Pi or −Pi medium for 2 d. GFP fluorescence was visualized by confocal microscopy. (d) Intensity of the GFP fluorescence (arbitrary units, au) in nuclei of the root tips. Data are means ± SD (*n* = 10 independent seedlings). Asterisk indicates significant difference (Tukey test, $P < 0.05$). (e) Western blot analysis. Four-day-old seedlings of WT plants were transferred to either +Pi or −Pi medium for 2 d with or without 50 μM MG132.

expression induction of Pi-deficiency-responsive genes should be activated in the *hdc1* mutant even under Pi-sufficient conditions. Keeping this point in mind, we found that Pi deficiency enhanced the expression of a number of root remodeling genes, including *LPR1*, *LPR2*, *ALMT1* and *PT2*, but not *PDR2* and *STOP1*, in the WT plants (Fig. 7a). However, in the *hdc1* mutant, except for *PDR2*, the expression of the others was significantly increased in comparison with the WT plants under Pi-deficiency conditions. It is interesting to note that the expression of two of the key genes involved in Pi deficiency-mediated root Fe uptake, *LPR1* and *ALMT1*, were two of the genes that appeared to be negatively regulated by WT HDC1.

To further confirm the negative effects of HDC1 on the expression regulation of *LPR1* and *ALMT1*, we performed promoter GUS activity analysis of *ALMT1* and *LPR1* in the WT and the *hdc1* mutant in response to Pi availability. We introduced *ALMT1pro::GUS* and *LPR1pro::GUS* into WT or *hdc1* plants, respectively. Although Pi deficiency resulted in the

increase of both *ALMT1* and *LPR1* promoter activities in root tips of the WT plants, as reflected by increased GUS staining, this increase was much stronger in the *hdc1* mutant plants (Fig. 7b). These results suggest that HDC1 negatively regulated the expression of *LPR1* and *ALMT1* under Pi deficiency.

HDC1 affects the level of H3 acetylation of genes involved in RSA remodeling under Pi deficiency

To investigate whether the increased expression of *ALMT1*, *LPR1* and *LPR2* in the *hdc1* mutants is related directly to the changes in the acetylation levels of histone H3 of *LPR1*, *LPR2* and *ALMT1*, we performed a ChIP-qPCR analysis. To check the quality of the ChIP-DNA, previously reported *PYL4* and *ABA3* were includedas positive and negative controls, respectively (Perrella *et al.*, 2013). Consistent with previous reports, transcript abundances of *PYL4* were more enriched in the *hdc1* mutants independent of Pi status (Fig. S6a). However, no change was
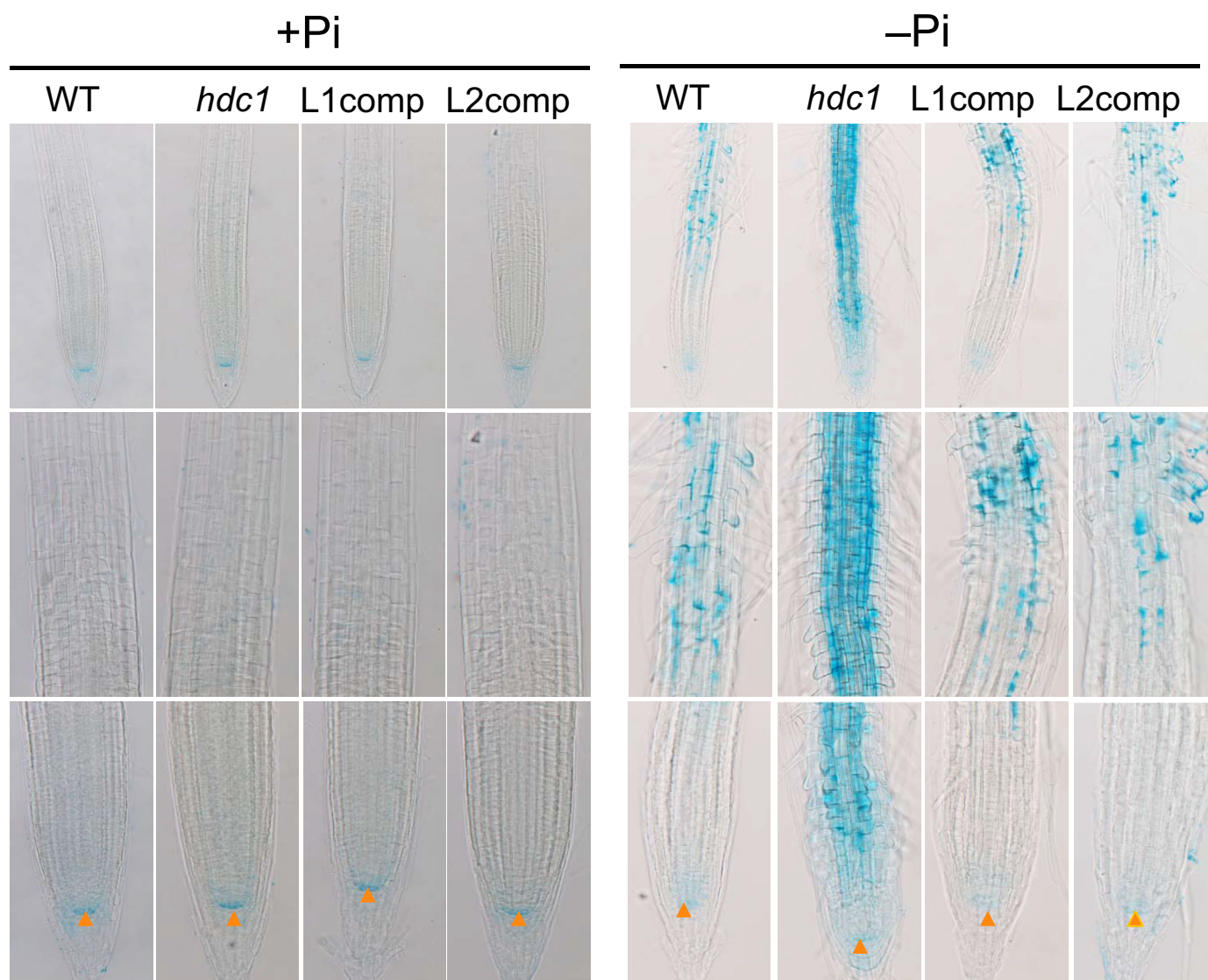
Fig. 4 *hdc1* overaccumulates Fe^{3+} in roots under inorganic phosphate (Pi) deficiency in *Arabidopsis thaliana*. Iron (Fe) accumulation patterns as indicated by Perls staining in the root apex of 4-d-old seedlings of wild-type (WT), *hdc1* and two complementation lines grown on Pi-sufficient medium (+Pi) or Pi-deficient medium (−Pi) for 2 d. Top panel, whole root tip; middle panel, higher magnification of maturation zone; bottom panel, higher magnification of apical region, including root cap, meristem and transition zone. Note the changes of accumulation of Fe in the SCN (orange arrowhead).

found for *ABA3* transcript abundance (Fig. S6b). Next, we selected four representative regions of each gene, that is, the promoter region (up), the transcription start site (5′), the gene body region (mid), and the site near the 3′ UTR (3′) (Fig. 8a). For *LPR1 and LPR2*, the H3 acetylation level was highest at 5′, whereas, for *ALMT1*, it was highest at the up (Fig. 8b). Compared with the WT plants, the histone H3 acetylation level of *LPR1* and *LPR2* was significantly higher at the 5′ region in the *hdc1* mutant irrespective of Pi status. Under Pi-deficient conditions, the histone H3 acetylation level at the up, 5′ and 3′ regions of *ALMT1* was higher in the *hdc1* mutant than in the WT plants. Overall, HDC1 negatively affected the H3 acetylation level of the genes involved in RSA remodeling under Pi deficiency. However, the changes in H3 acetylation in *ALMT1* were much less than those of *LPR1* and *LPR2*. Therefore, it remains that the transcriptional changes of *ALMT1* may be the consequences of

increased Fe accumulation in the *hdc1* mutant, as recent evidence showed that Fe is sufficient to trigger the accumulation of STOP1 in the nucleus, which in turn regulates *ALMT1* expression (Godon *et al.*, 2019).

HDC1 acts upstream of LPR1/2

In *Arabidopsis*, LPR1 and its homolog LPR2 are epistatic to other identified components regulating the Pi deficiency-induced inhibition of primary root growth (Svistoonoff *et al.*, 2007). To study the genetic relationship between *HDC1* and *LPR1*, we first developed an *hdc1/lpr1* double mutant. Consistent with previous reports, we found that *lpr1* was insensitive to Pi deficiency-induced root growth inhibition (Fig. 9a). Whereas *hdc1* exhibited hypersensitivity to Pi deficiency, the *hdc1/lpr1*double mutant was insensitive to Pi deficiency, a phenomenon resembling that of the
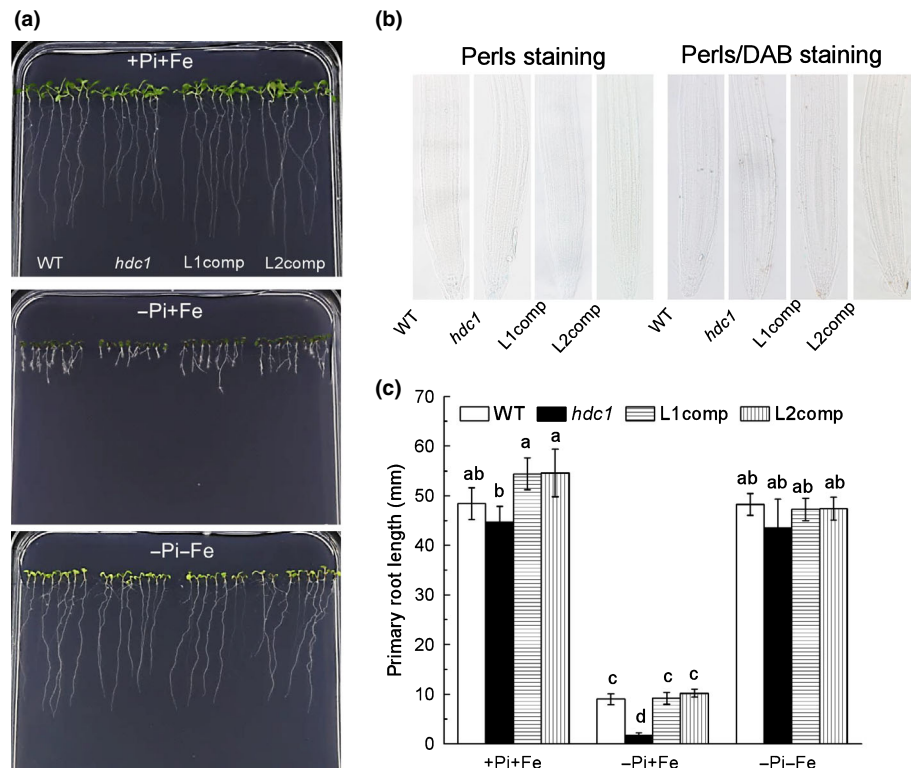
Fig. 5 Iron (Fe) dependence of the inhibition of primary root growth under inorganic phosphate (Pi) deficiency in *Arabidopsis thaliana*. (a) Phenotype of 7-d-old seedlings of wild-type (WT), *hdc1* and complementation lines grown on +Pi+Fe, −Pi+Fe, or −Pi−Fe medium. (b) Perls and Perls/diaminobenzidine (DAB) staining of Fe in root tip of 3-d-old seedlings of WT, *hdc1* and complementation lines. (c) Primary root length of seedling in (a). Data are means ± SD (n = 8). Different letters indicate significant differences (Tukey test, $P < 0.05$).

lpr1 mutant. In addition, the Pi deficiency-induced increase in root hair density was much less in the *hdc1/lpr1* double mutant than in the WT and *hdc1*, which is again similar to the *lpr1* mutant (Fig. 9b). Moreover, the *hdc1/lpr1* double mutant root tip exhibited diminished localized root Fe deposition, which is consistent with *lpr1* (Fig. 9d). However, primary root growth in the *hdc1/lpr1* double mutant was not completely recovered (Fig. 9c), suggesting the functional redundancy of LPR2 to LPR1. We thus developed the *hdc1/lpr1/lpr2* triple mutant. As expected, there were no differences in primary root growth between the *hdc1/lpr1/lpr2* triple mutants and *lpr1/lpr2* double mutants (Fig. S7). These results indicate that HDC1 acts upstream of LPR1/2 to participate in root architecture remodeling under Pi deficiency.

Discussion

The modifications of RSA that improve a plant's ability to explore the top layers of the soil where Pi tends to accumulate is a major developmental response of plants to Pi deficiency (Lopez-Bucio *et al.*, 2003). In the present study, we characterized the *Arabidopsis* mutant *hdc1* as being hypersensitive to the inhibition of primary root growth, to the stimulation of lateral root production, and to the increase in root hair density under Pi-deficiency conditions (Figs 1, S3). A previous study showed that *hdc1* knockout mutants had higher levels of the acetylated form of H3 than of the deacetylated form in comparison with WT plants (Perrella *et al.*, 2013). The current finding that Pi deficiency
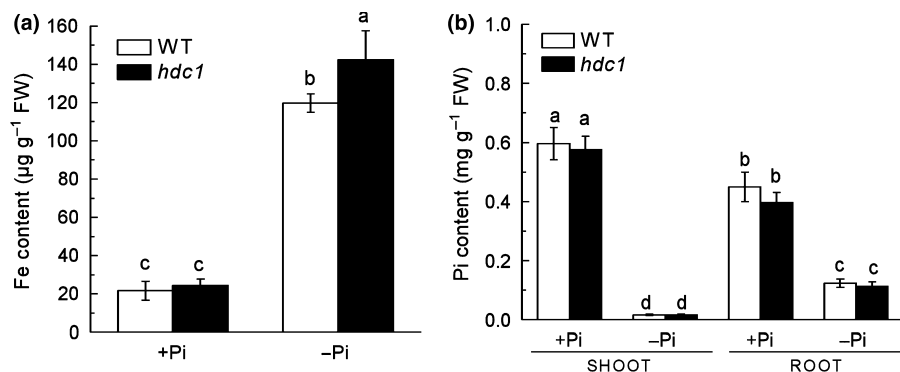
Fig. 6 Iron (Fe) content and inorganic phosphate (Pi) content in wild-type (WT) and *hdc1* mutant *Arabidopsis thaliana* plants. (a) Fe content in roots of WT and *hdc1*. Seven-day-old seedlings were grown on +Pi or −Pi medium for 7 d. Roots were harvested for Fe content determination. Data are means ± SD (n = 8). Different letters indicate significant differences (Tukey test, $P < 0.05$). (b) Pi content in roots and shoot of WT and *hdc1* mutant plants. Seven-day-old seedlings were grown on +Pi or −Pi medium for 7 d. Roots and shoots were harvested separately for Fe content determination. Data are means ± SD (n = 8). Different letters indicate significant differences (Tukey test, $P < 0.05$).

(a)

(b)
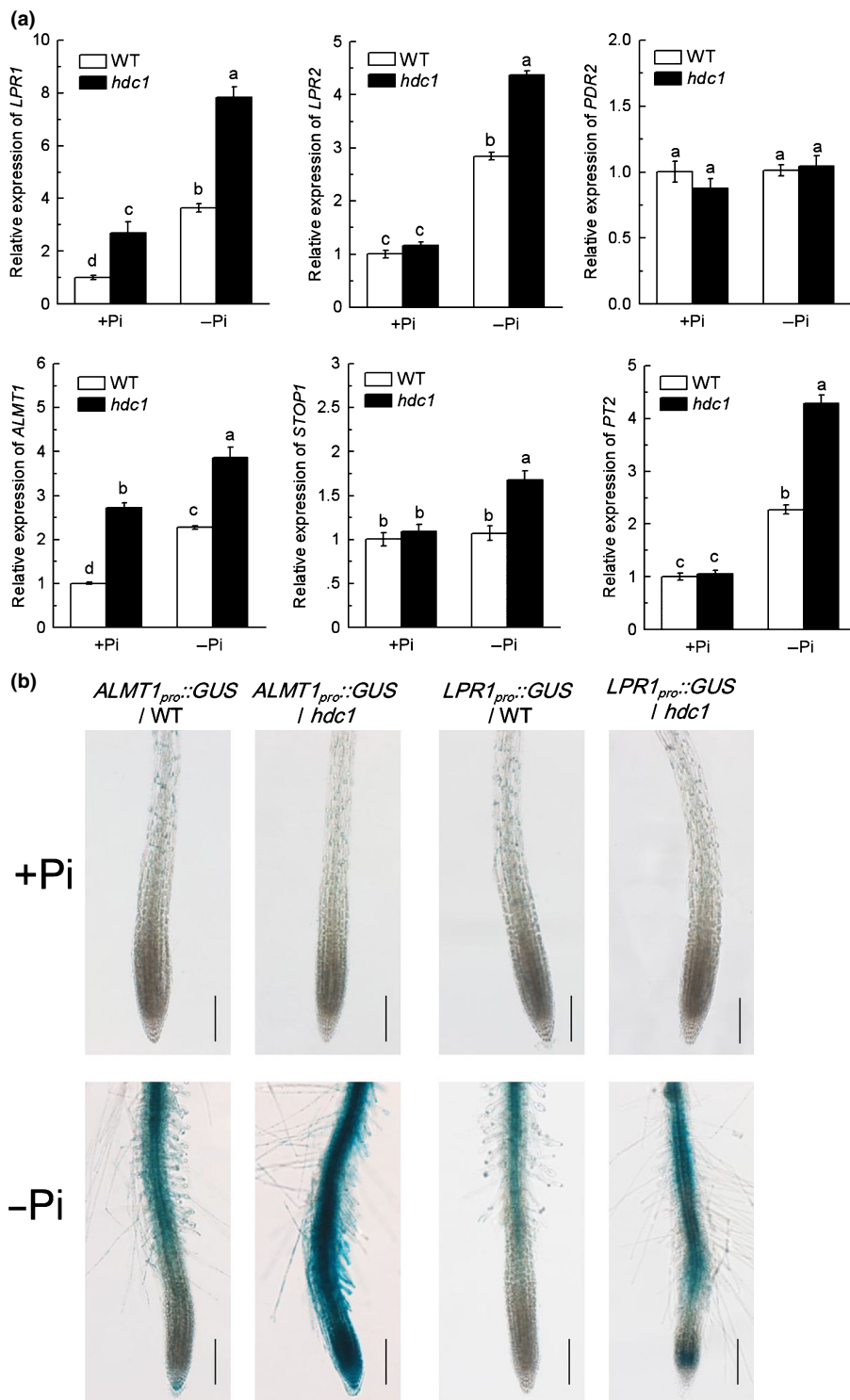
Fig. 7 HDC1 negatively regulates expression of genes involved in root system architecture remodeling under inorganic phosphate (Pi) deficiency in *Arabidopsis thaliana*. (a) Quantitative reverse transcription polymerase chain reaction (qRT-PCR) analysis. Four-day-old seedlings of wild-type (WT) and *hdc1* were grown on Pi-sufficient (+Pi) or -deficient (−Pi) medium for 2 d. The apical 3 mm of roots were excised for RNA extraction and qRT-PCR analysis. Expression level was normalized to the expression of an internal control, *AtACT2*. Data are means ± SD ($n = 8$). Different letters indicate significant differences (Tukey test, $P < 0.05$). (b) β-Glucuronidase (GUS) activity assays for expression pattern of *ALMT1* and *LPR1* in WT and *hdc1* backgrounds under Pi-sufficiency or -deficiency conditions. Bars, 200 μm.

resulted in the accumulation of acetylated H3 (Fig. 1a) is consistent with the post-transcriptional downregulation of *HDC1* (Fig. 3), which is a core component of the HDAC complex (Perrella *et al.*, 2013). These results suggest that modifications of histone acetylation play roles in Pi deficiency-induced RSA remodeling in *Arabidopsis*. In recent years, accumulating evidence has suggested that chromatin modification plays important roles in nutrient stresses (Secco *et al.*, 2017). Thus, our present results

provide another line of evidence linking chromatin modifications with plant Pi nutrition in *Arabidopsis* plants.

HDC1 is a core component of the HDAC complex and can interact with HDA6 and HDA19 to regulate the activity of histone deacetylases (Perrella *et al.*, 2013), suggesting that the function of HDC1 is closely related to its interacting partners. It has been demonstrated that *hdc1*, *hda6* and *hda19* share several common phenotypes such as abscisic acid-sensitive
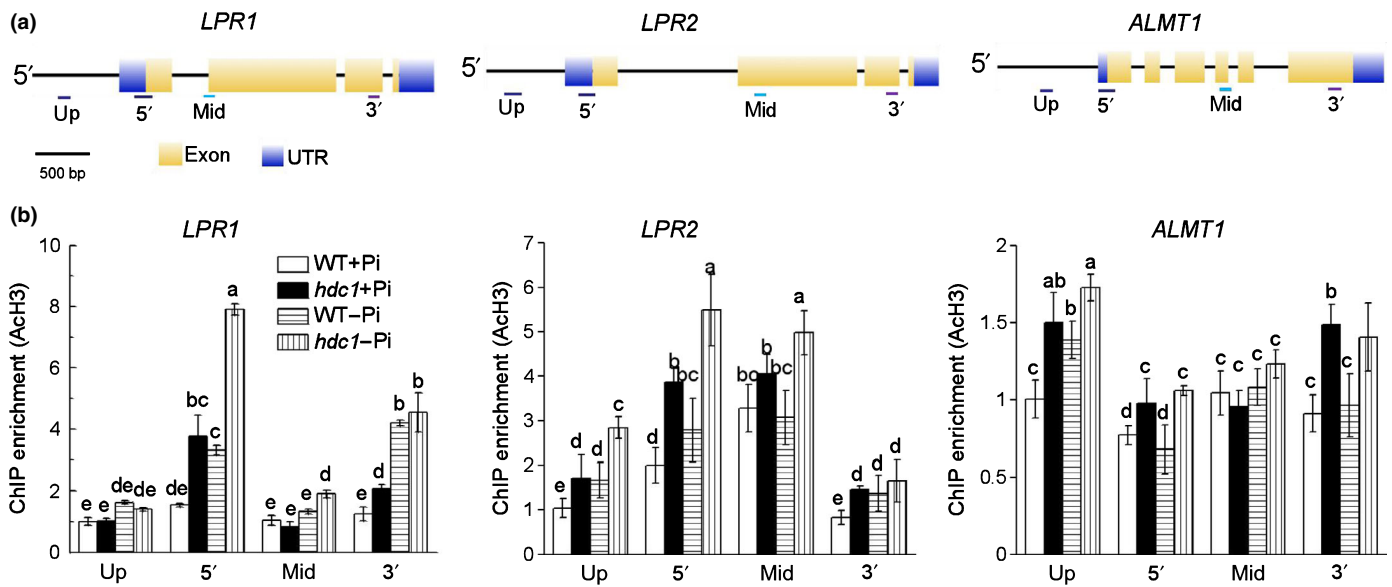
Fig. 8 HDC1 negatively affects H3 acetylation status of *ALMT1*, *LPR1* and *LPR2*. (a) Schematic diagram showing the genomic structure of *LPR1*, *LPR2* and *ALMT1*. (b) H3 acetylation of *ALMT1*, *LPR1* and *LPR2*. Relative H3 acetylation was determined by chromatin immunoprecipitation (ChIP) assays and normalized to input DNA (chromatin before immunoprecipitation). The value of wild-type (WT) under inorganic phosphate-sufficient (+Pi) conditions was arbitrarily given as 1. Data are means ± SD ($n = 3$). Different letters indicate significant differences (Tukey test, $P < 0.05$).

germination and flowering (Song *et al.*, 2005; Yu *et al.*, 2011) and reduced vegetative growth (Perrella *et al.*, 2013). However, we found that the involvement of HDC1 in Pi-deficiency responses is different from that of HDA19 or HDA6 in *Arabidopsis*, although HDC1 could interact with either HDA6 or HDA19 to promote histone deacetylation (Perrella *et al.*, 2013). This conclusion is supported by the following lines of evidence. First, HDA6 and HDA19 were shown to control epidermal cell length, thereby affecting root hair density and length in response to Pi deficiency (Chen *et al.*, 2015). By contrast, HDC1 is largely involved in the inhibition of primary root growth with a secondary effect on root hair density under Pi deficiency (Fig. 1). Second, HDA19 affects the transcription of genes encoding SPX (SYG1/Pho81/XPR) domain-containing proteins and genes involved in membrane lipid remodeling, a key response to Pi starvation that increases the free Pi in plants (Chen *et al.*, 2015). However, HDC1 is involved in transcriptional repression of genes involved in the local responses to Pi deficiency (Fig. 8). Therefore, HDC1 plays roles distinct from HDA6 or HDA19. This conclusion was further supported by the fact that *hdc1* did not phenocopy the aberrant developmental phenotypes of the *hda6 hda19* double mutants (Tian & Chen, 2001; Tanaka *et al.*, 2008).

In yeast and mammals, HDACs operate within multiprotein complexes (Yang & Seto, 2008). Although plant HDAC complexes are less well characterized, a recent study suggested that the basic composition of plant HDAC complexes is similar to that of animal and yeast complexes (Mehdi *et al.*, 2016). A quantitative bimolecular fluorescence complementation assay in tobacco (*Nicotiana benthamiana*) epidermal cells has revealed that HDC1 can interact not only with HDAs (HDA6 and HDA19) but also with the histone-binding proteins SHL1, ING2 and MSI1, the

Sin3-associated protein SAP18, and H1 variants. However, HDC1 could not interact with the Sin3-like (SNL) corepressors SNL2 and SNL3 (Perrella *et al.*, 2016). Taking these findings and our results together, we propose that HDC1 regulates different Pi-deficiency responses from those of HDA19. However, the mechanisms of how HDC1 regulates the histone deacetylation of genes involved in root tip Fe homeostasis must be investigated in future.

We demonstrated that HDC1 is involved in local responses to Pi deficiency in *Arabidopsis*. Local responses are processes including the inhibition of primary root growth, enhancement of lateral root density, and increases in the number and length of root hairs (Bates & Lynch, 1996), all of which are triggered by the Pi concentration in the soil around the root tip and are independent of internal Pi concentrations (Thibaud *et al.*, 2010). Here, we found that in the *hdc1* mutant, primary root growth ceased on day 2 of Pi deficiency and also exhibited increased root hair density (Figs 1, 2, S3), which are hallmarks of local responses to Pi deficiency in *Arabidopsis* (Abel, 2017). Root tip growth inhibition depends on local Pi, but systemic responses involving intracellular Pi sensing also occur and are controlled by the overall plant Pi concentration. The finding that there are no differences in the shoot and root Pi contents between the *hdc1* and WT plants (Fig. 6) indicated that HDC1 may not be a major modulator of systemic responses to Pi deficiency. It is noteworthy that some Pi deficiency-responsive genes other than those involved in local responses were also regulated by HDC1 under Pi-deficient conditions. For example, the expression of *PT2* was significantly higher in the *hdc1* mutant than in the WT under Pi-deficient conditions (Fig. 7). One possible explanation for this is that the increased expression of PT2 was the consequence of increased sensitivity of *hdc1* to Pi deficiency.
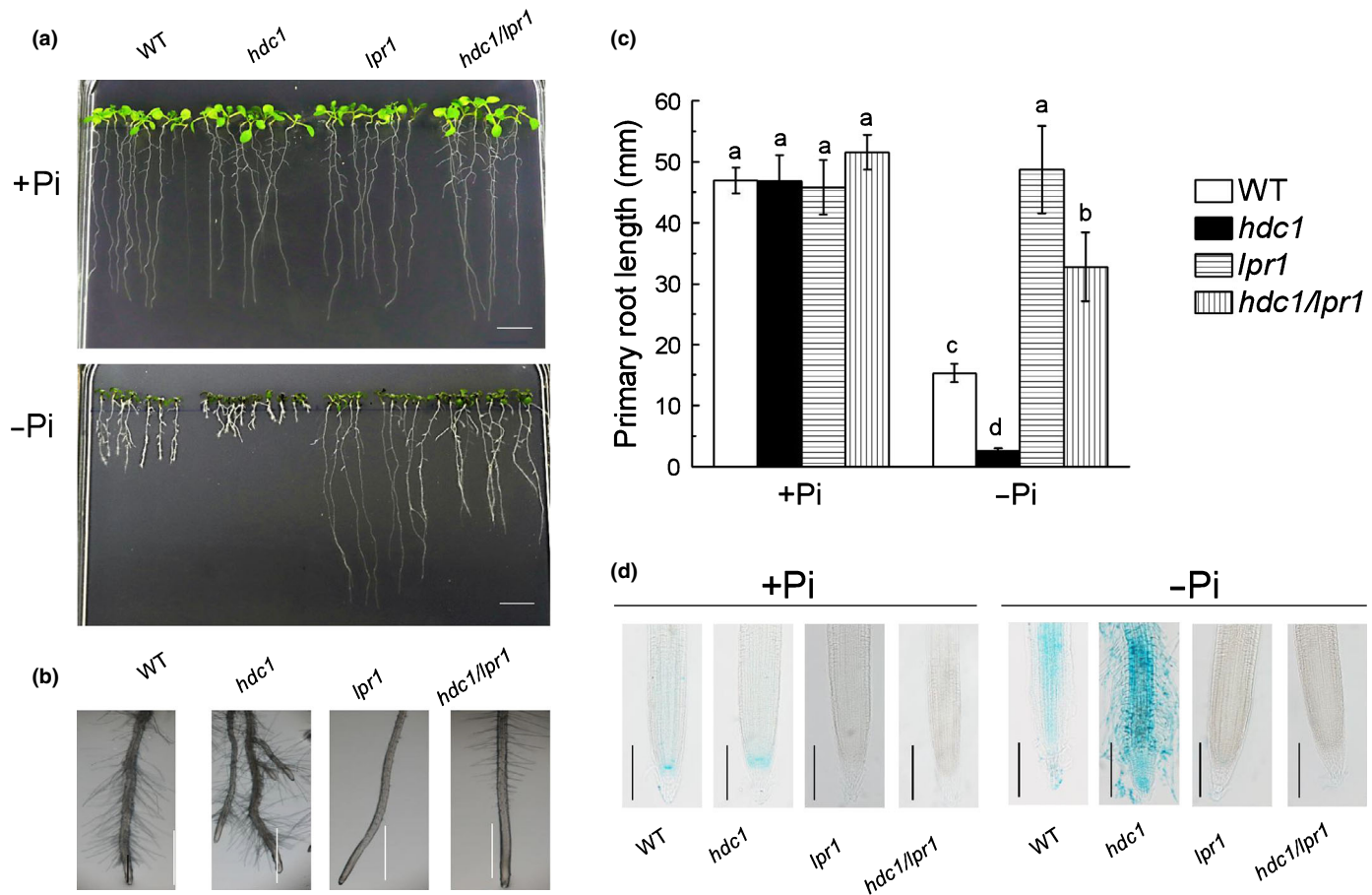
Fig. 9 HDC1 acts upstream of LPR1 to regulate inorganic phosphate (Pi) deficiency responses in Arabidopsis. (a) Phenotype of 7-d-old seedlings of wild-type (WT), *hdc1*, *lpr1* and *hdc1/lpr1* double mutants grown on inorganic phosphate-sufficient (+Pi) or -insufficient (−Pi) medium. Bars, 1 cm. (b) Close-up view of the morphology of the primary root of the seedlings in (a). Bars, 1 cm. (c) Primary root length of the seedlings in (a). Data are means ± SD ($n = 8$). Different letters indicate significant differences (Tukey test, $P < 0.05$). (d) Perls staining of iron (Fe) accumulation in root tips of 4-d-old seedlings grown on +Pi or −Pi medium for 3 d. Bars, 200 μm.

Phosphate deficiency-induced root tip inhibition requires Fe and involves LPR1 and LPR2 ferroxidases, leading to apoplastic Fe^{3+} accumulation and a concomitant increase in ROS and callose deposition in the root meristem (Svistoonoff *et al.*, 2007). Here, we demonstrated that *hdc1* increases the inhibition of primary root growth, which could be attributed to the increased Fe accumulation in the root tip. This is supported by the following findings. First, Perls staining results showed that the RAM, elongation and maturation zones accumulated more Fe in the *hdc1* mutant than in WT plants under Pi deficiency conditions (Figs 4, S5). Second, the observed Pi deficiency-induced root tip Fe accumulation and root growth inhibition were dependent on the presence of exogenous Fe in the growth medium (Fig. 5). Third, in the *hdc1/lpr1* double mutant, neither the Pi-hypersensitive phenotype nor the overaccumulation of Fe^{3+} was observed (Fig. 9). Finally, qRT-PCR analysis revealed that HDC1 negatively regulated the transcription of *ALMT1*, *STOP1*, *LPR1* and *LPR2*, and these are all genes involved in Fe homeostasis in the root tip under Pi deficiency (Fig. 7). In eukaryotes, the efficiency of gene transcription is ultimately determined by the higher-order structure of chromatin (Berger, 2007).

Therefore, it can be envisioned that the increased acetylation of histone H3 in the *hdc1* mutants establishes an active mark for gene transcription of these genes.

Previous studies indicated that histone acetylation can occur in both the proximal promoter and/or exons (Benhamed *et al.*, 2006). Our ChIP-qPCR analysis showed that there was increased H3 acetylation in *ALMT1*, *LPR1* and *LPR2* in response to Pi deficiency (Fig. 8), which is consistent with the accumulation of acetylated histone H3 in response to Pi deficiency (Figs 1, S1). Compared with the WT plants, the *hdc1* mutant plants exhibited increased H3 acetylation in *ALMT1*, *LPR1* and *LPR2*, even under Pi-sufficiency conditions, suggesting that HDC1 itself represses the histone acetylation of these genes. These findings lead us to propose a hypothetical model to illustrate the mechanism of HDC1-mediated Pi-deficiency responses in Arabidopsis. Pi deficiency post-transcriptionally regulates HDC1 to suppress its protein abundance, possibly via the 26S proteasome pathway, which results in increased histone H3 acetylation of some Pi deficiency-induced genes involved in root tip Fe homeostasis. The increased acetylation triggers the transcriptional expression of these genes, which ultimately causes the primary root growth inhibition.

Acknowledgements

Author contributions

JLY and SJZ designed the research. JMX, ZQW and JYW performed the research. PFL, JFJ, WWC and WF provided experimental assistance. JMX, ZQW and JLY analyzed the data. JLY, SJZ and LVK wrote the article.

ORCID

Leon V. Kochian (iD) https://orcid.org/0000-0003-3416-089X
Jian Li Yang (iD) https://orcid.org/0000-0003-0385-5787
Shao Jian Zheng (iD) https://orcid.org/0000-0002-3336-8165

References

Abel S. 2017. Phosphate scouting by root tips. *Current Opinion in Plant Biology* **39**: 168–177.

Balzergue C, Dartevelle T, Godon C, Lauqier E, Meisrimler C, Teulon JM, Creff A, Bissler M, Brouchoud C, Haqèqe A *et al.* 2017. Low phosphate activates STOP1-ALMT1 to rapidly inhibit root cell elongation. *Nature Communications* **8**: 15300.

Bates TR, Lynch JP. 1996. Stimulation of root hair elongation in *Arabidopsis thaliana* by low phosphorus availability. *Plant, Cell & Environment* **19**: 529–538.

Belal R, Tang R, Li Y, Mabrouk Y, Badr E, Luan S. 2015. An ABC transporter complex encoded by Aluminum Sensitive 3 and NAP3 is required for phosphate deficiency responses in Arabidopsis. *Biochemical and Biophysical Research Communications* **463**: 18–23.

Benhamed M, Bertrand C, Servet C, Zhou DX. 2006. Arabidopsis GCN5, HD1, and TAF1/HAF2 interact to regulate histone acetylation required for light-responsive gene expression. *Plant Cell* **18**: 2893–2903.

Berger SL. 2007. The complex language of chromatin regulation during transcription. *Nature* **447**: 407–412.

Buston R, Castrillo G, Linhares F, Puga MI, Rubio V, Perez-Perez J, Solano R, Leyva A, Paz-Ares J. 2010. A central regulatory system largely controls transcriptional activation and repression responses to phosphate starvation in Arabidopsis. *PLoS Genetics* **6**: e1001102.

Chen CY, Wu K, Schmidt W. 2015. The histone deacetylase HDA19 controls root cell elongation and modulates a subset of phosphate starvation responses in Arabidopsis. *Scientific Reports* **5**: 15708.

Chen J, Liu Y, Ni J, Wang Y, Bai Y, Shi J, Gan J, Wu Z, Wu P. 2011. OsPHF1 regulates the plasma membrane localization of low-and high-affinity inorganic phosphate transporters and determines inorganic phosphate uptake and translocation in rice. *Plant Physiology* **157**: 269–278.

Chen YF, Li LQ, Xu Q, Kong YH, Wang H, Wu WH. 2009. The WRKY6 transcription factor modulates *PHOSPHATE1* expression in response to low Pi stress in *Arabidopsis*. *Plant Cell* **21**: 3554–3566.

Delhaize E, Randall PJ. 1995. Characterization of a phosphate-accumulator mutant of Arabidopsis thaliana. *Plant Physiology* **107**: 207–213.

Devaiah BN, Karthikeyan AS, Raghothama KG. 2007. WRKY75 transcription factor is a modulator of phosphate acquisition and root development in Arabidopsis. *Plant Physiology* **143**: 1789–1801.

Dong J, Piñeros MA, Li X, Yang H, Liu Y, Murphy AS, Kochian LV, Liu D. 2017. An *Arabidopsis* ABC transporter mediates phosphate deficiency-induced remodeling of root architecture by modulating iron homeostasis in roots. *Molecular Plant* **10**: 244–259.

Gendrel AV, Lippman Z, Martienssen R, Colot V. 2005. Profiling histone modification patterns in plants using genomic tiling microarrays. *Nature Methods* **2**: 213.

Godon C, Mercier C, Wang X, David P, Richaud P, Nussaume L, Liu D, Desnos T. 2019. Under phosphate starvation conditions, Fe and Al trigger accumulation of the transcription factor STOP1 in the nucleus of Arabidopsis root cells. *The Plant Journal* **99**: 937–949.

Gutiérrez-Alanís D, Ojeda-Rivera JO, Yong-Villalobos L, Cárdenas-Torres L, Herrera-Estrella L. 2018. Adaptation to phosphate scarcity: tips from *Arabidopsis* roots. *Trends in Plant Science* **23**: 721–730.

Hergeth SP, Schneider R. 2015. The H1 linker histones: multifunctional proteins beyond the nucleosomal core particle. *EMBO Reports* **16**: 1439–1453.

Holford ICR. 1997. Soil phosphorus: its measurement, and its uptake by plants. *Australian Journal of Soil Research* **35**: 227–240.

Iuchi S, Koyama H, Kobayashi Y, Kitabayashi S, Kobayashi S, Ikka T, Hirayama T, Shinozaki K, Kobayashi M. 2007. Zinc finger protein STOP1 is critical for proton tolerance in Arabidopsis and coregulates a key gene in aluminum tolerance. *Proceedings of the National Academy of Sciences, USA* **104**: 9900–9905.

Jefferson RA, Kavanagh TA, Bevan MW. 1987. GUS fusions: beta-glucuronidase as a sensitive and versatile gene fusion marker in higher plants. *EMBO Journal* **6**: 3901–3907.

Kouzarides T. 2007. Chromatin modifications and their function. *Cell* **128**: 693–705.

Kuo HF, Chang TY, Chiang SF, Wang WD, Charng YY, Chiou TJ. 2014. Arabidopsis inositol pentakisphosphate 2-kinase, AtIPK1, is required for growth and modulates phosphate homeostasis at the transcriptional level. *The Plant Journal* **80**: 503–515.

Laemmli UK. 1970. Cleavage of structural proteins during the assembly of the head of bacteriophage T4. *Nature* **227**: 680–685.

Lopez-Bucio J, Cruz-Ramirez A, Herrera-Estrella L. 2003. The role of nutrient availability in regulating root architecture. *Current Opinion in Plant Biology* **6**: 280–287.

Marschner H. 1995. *Mineral nutrition of higher plants.* London, UK: Academic Press.

Meguro R, Asano Y, Odagiri S, Li C, Iwatsuki H, Shoumura K. 2007. Nonheme-iron histochemistry for light and electron microscopy: a historical, theoretical and technical review. *Archives of Histology and Cytology* **70**: 1–19.

Mehdi S, Derkacheva M, Ramström M, Kralemann L, Bergquist J, Hennig L. 2016. The WD40 domain protein MSI1 functions in a histone deacetylase complex to fine-tune abscisic acid signaling. *Plant Cell* **28**: 42–54.

Mora-Macías J, Ojeda-Rivera JO, Gutiérrez-Alanís D, Yong-Villalobos L, Oropeza-Aburto A, Raya-González J, Jiménez-Domínquez G, Chávez-Calvillo G, Rellán-Álvarez R, Herrera-Estrella L. 2017. Malate-dependent Fe accumulation is a critical checkpoint in the root developmental response to low phosphate. *Proceedings of the National Academy of Sciences, USA* **114**: E3563–E3572.

Over RS, Michaels SD. 2014. Open and closed: the roles of linker histones in plants and animals. *Molecular Plant* **7**: 481–491.

Perrella G, Carr C, Asensi-Fabado MA, Donald NA, Páldi K, Hannah MA, Amtmann A. 2016. The histone deacetylase complex 1 protein of Arabidopsis has the capacity to interact with multiple proteins including histone 3-binding proteins and histone variants. *Plant Physiology* **171**: 62–70.

Perrella G, Lopez-Vernaza MA, Carr C, Sani E, Gosselé V, Verduyn C, Kellermeier F, Hannah MA, Amtmann A. 2013. Histone deacetylase comlex1 expression level titrates plant growth and abscisic acid sensitivity in Arabidopsis. *Plant Cell* **25**: 3491–3505.

Roschzttardtz H, Conejero G, Curie C, Mari S. 2009. Identification of the endodermal vacuole as the iron storage compartment in the Arabidopsis embryo. *Plant Physiology* **151**: 1329–1338.

Roudier F, Teixeira FK, Colot V. 2009. Chromatin indexing in Arabidopsis: An epigenomic tale of tails and more. *Trends in Genetics* **25**: 511–517.

Sánchez-Calderón L, Lópze-Bucio J, Chacón-López A, Cruze-Ramíez A, Nieto-Jacobo F, Dubrovsky JG, Herrera-Estrella L. 2005. Phosphate starvation

induces a determinate developmental program in the roots of *Arabidopsis thaliana*. *Plant Cell Physiology* **46**: 174–184.

Secco D, Whelan J, Rouached H, Lister R. 2017. Nutrient stress-induced chromatin changes in plants. *Current Opinion in Plant Biology* **39**: 1–7.

Smith AP, Jain A, Deal RB, Nagarajan VK, Poling MD, Raghothama KG, Meagher RB. 2010. Histone H2A.Z regulates the expression of several classes of phosphate starvation response genes but not as a transcriptional activator. *Plant Physiology* **152**: 217–225.

Song CP, Agarwal M, Ohta M, Guo Y, Halfter U, Wang P, Zhu JK. 2005. Role of an Arabidopsis AP2/EREBP-type transcriptional repressor in abscisic acid and drought stress responses. *Plant Cell* **17**: 2384–2396.

Su T, Zhang FC, Chen Y, Li LQ, Wu WH, Chen YF. 2015. WRKY42 modulates phosphate homeostasis through regulating phosphate translocation and acquisition in Arabidopsis. *Plant Physiology* **167**: 1579–1591.

Svistoonoff S, Creff A, Reymond M, Sigoillot-Claude C, Ricaud L, Blanchet A, Nussaume L, Desnos T. 2007. Root tip contact with low-phosphate media reprograms plant root architecture. *Nature Genetics* **39**: 792.

Tanaka M, Kikuchi A, Kamada H. 2008. The Arabidopsis histone deacetylases HDA6 and HDA19 contribute to the repression of embryonic properties after germination. *Plant Physiology* **146**: 149–161.

Thibaud MC, Arrighi JF, Bayle V, Chiarenza S, Creff A, Bustos R, Paz-Ares J, Poirier Y, Nussaume N. 2010. Dissection of local and systemic transcriptional responses to phosphate starvation in Arabidopsis. *The Plant Journal* **64**: 775–789.

Tian L, Chen ZJ. 2001. Blocking histone deacetylation in Arabidopsis induces pleiotropic effects on plant gene regulation and development. *Proceedings of the National Academy of Sciences, USA* **98**: 200–205.

Ticconi CA, Delatorre CA, Lahner B, Salt DE, Abel S. 2004. Arabidopsis *pdr2* reveals a phosphate-sensitive checkpoint in root development. *The Plant Journal* **37**: 801–814.

Tokizawa M, Kobayashi Y, Saito T, Kobayashi M, Iuchi S, Nomoto M, Tada Y, Yamamoto YY, Koyama H. 2015. Sensitive to proton rhizotoxicity1, calmodulin binding transcription activator2, and other transcription factors are involved in aluminum-activated malate transporter1 expression. *Plant Physiology* **167**: 991–1003.

Wang H, Xu Q, Kong YH, Chen Y, Duan JY, Wu WH, Chen YF. 2014. Arabidopsis WRKY45 transcription factor activates *PHOSPHATE TRANSPORTER1;1* expression in response to phosphate starvation. *Plant Physiology* **164**: 2020–2029.

Ward JT, Lahner B, Yakubova E, Salt DE, Raghothama KG. 2008. The effect of iron on the primary root elongation of Arabidopsis during phosphate deficiency. *Plant Physiology* **147**: 1181–1191.

Xu JM, Wang ZQ, Jin JF, Chen WW, Fan W, Zheng SJ, Yang JL. 2019. FeSTAR2 interacted by FeSTAR1 alters its subcellular location and regulates Al tolerance in buckwheat. *Plant and Soil* **436**: 489–501.

Yang XJ, Seto E. 2008. The Rpd3/Hda1 family of lysine deacetylases: from bacteria and yeast to mice and men. *Nature Reviews Molecular Cell Biology* **9**: 206–218.

Yu CW, Liu X, Luo M, Chen C, Lin X, Tian G, Lu Q, Cui Y, Wu K. 2011. HISTONE DEACETYLASE6 interacts with FLOWERING LOCUS D and regulates flowering in Arabidopsis. *Plant Physiology* **156**: 173–184.

Zheng SJ, Yang JL, He YF, Yu XH, Zhang L, You JF, Shen RF, Matsumoto H. 2005. Immobilization of aluminum with phosphorus in roots is associated with high aluminum resistance in buckwheat. *Plant Physiology* **138**: 297–303.

Supporting Information

Additional Supporting Information may be found online in the Supporting Information section at the end of the article.

Fig. S1 Western blot analysis of histone H3 and H4 acetylation of Arabidopsis roots subjected to Pi-sufficient (+Pi) or -deficient (–Pi) conditions.

Fig. S2 Western blot analysis of histone H3 acetylation in the roots of wild-type (WT) and two complementation lines subjected to Pi-sufficient (+Pi) or -deficient (–Pi) conditions for 2 d.

Fig. S3 HDC1 negatively affects root hair formation under Pi starvation in Arabidopsis.

Fig. S4 Relative primary root elongation of the WT and *hdc1* mutants in response to Pi deficiency.

Fig. S5 Fe accumulation patterns as indicated by Perls/DAB staining in the root apex of 4-day-old seedlings of the WT, *hdc1* and two complementation lines grown on Pi-sufficient medium (+Pi) or Pi-deficient medium (-Pi) for 2 d.

Fig. S6 HDC1affects histone H3 acetylation levels in *PYL4* but not in ABA3.

Fig. S7 Root phenotype of the WT, *hdc1*, *lpr1/lpr2* and *hdc1/lpr1/lpr2* plants grown under Pi-sufficient or -deficient conditions.

Table S1 Primers used in this study.

Please note: Wiley Blackwell are not responsible for the content or functionality of any Supporting Information supplied by the authors. Any queries (other than missing material) should be directed to the *New Phytologist* Central Office.